Zn- and Mg- Containing Tricalcium Phosphates-Based Adjuvants for Cancer Immunotherapy

Xiupeng Wang, Xia Li, Kazuo Onuma, Yu Sogo, Tadao Ohno, Atsuo Ito

Table S1. Zn to Ca mol ratio in Zn1, Zn1.5, Zn3, Zn6.8 and Mg to Ca mol ration in Mg1, Mg1.5, Mg3, Mg6.8

Samples	Zn to Ca mol ratio	Mg to Ca mol ratio
Zn1	0.93%±0.01%	-
Zn1.5	1.32%±0.03%	-
Zn3	2.91%±0.02%	-
Zn6.8	6.40%±0.02%	-
Mg1	-	0.88%±0.1%
Mg1.5	-	1.49%±0.02%
Mg3	-	2.98%±0.05%
Mg6.8	-	6.52%±0.05%

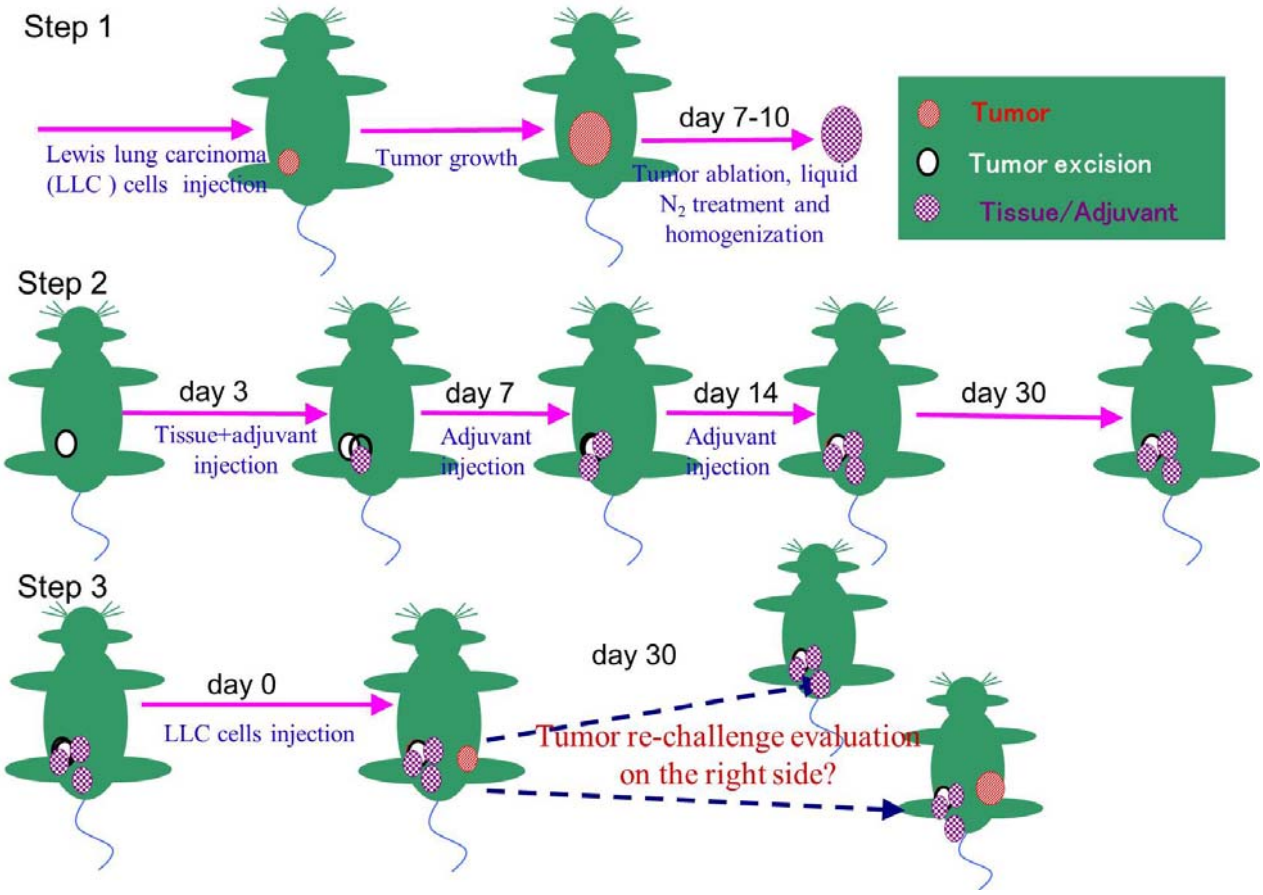

Figure S1. Scheme for the *in vivo* immunogenic activity evaluation

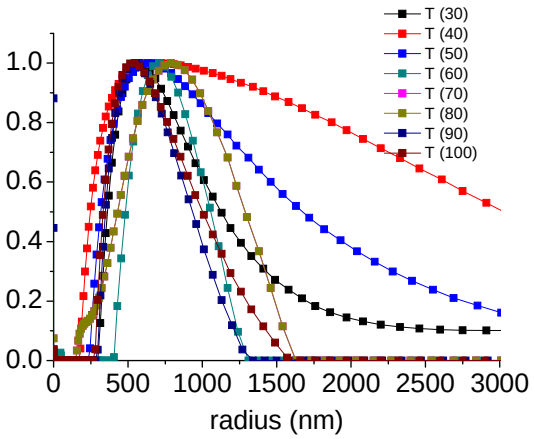

Figure S2. Distributions of hydrodynamic radius of TCP particles by dynamic light scattering measurement at various incidence angles of laser (from 30-100^{o})

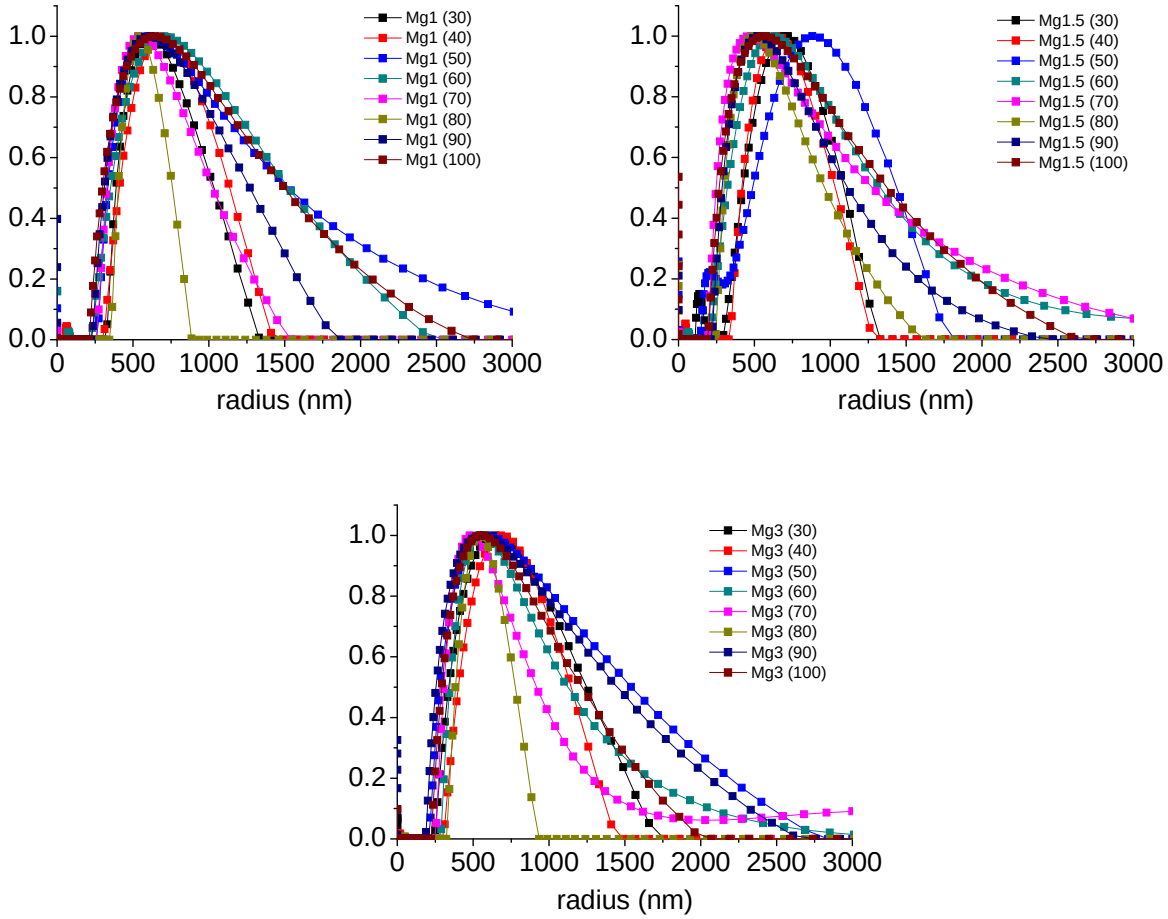

Figure S3. Distributions of hydrodynamic radius of Mg-TCP particles (Mg1, Mg1.5, Mg3) by dynamic light scattering measurement at various incidence angles of laser (from 30-100^{o})

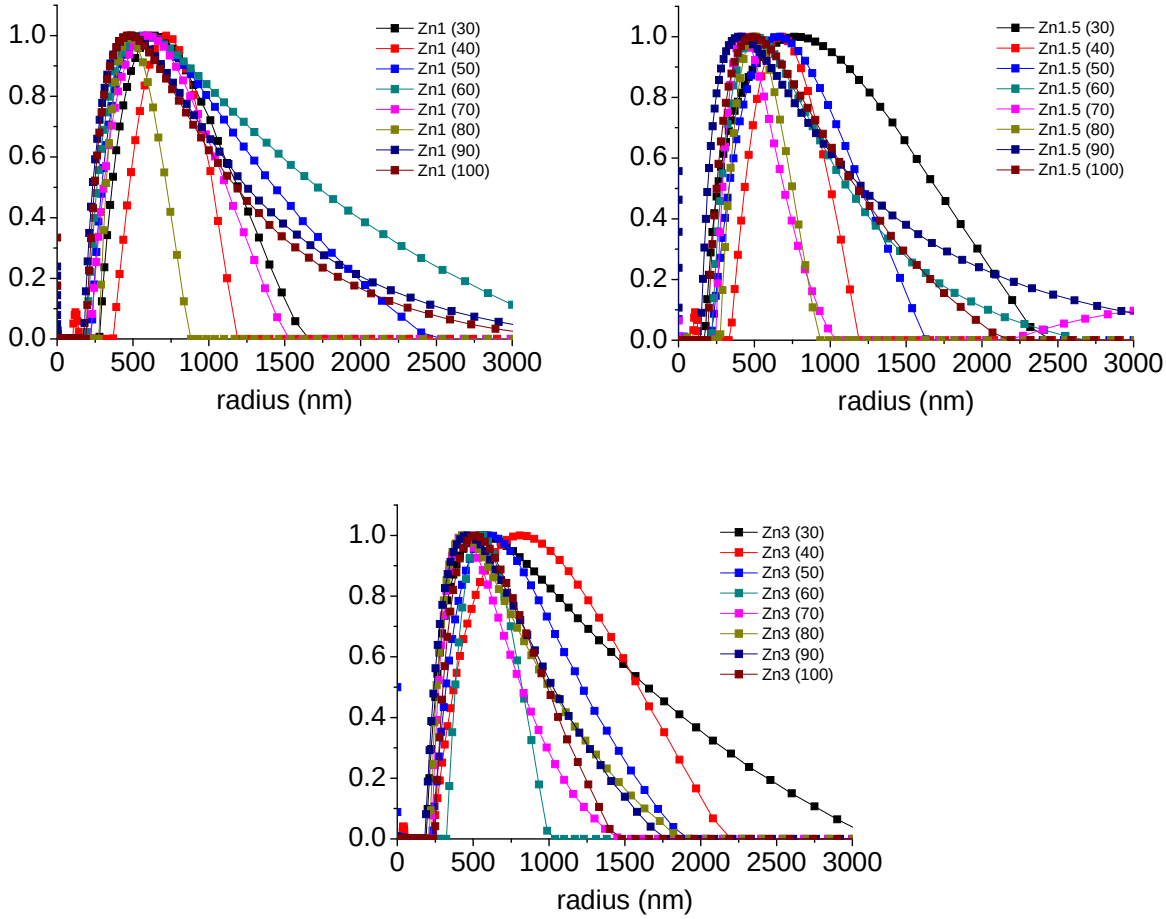

Figure S4. Distributions of hydrodynamic radius of Zn-TCP (Zn1, Zn1.5, Zn3) particles by dynamic light scattering measurement at various incidence angles of laser (from 30-100^{o})

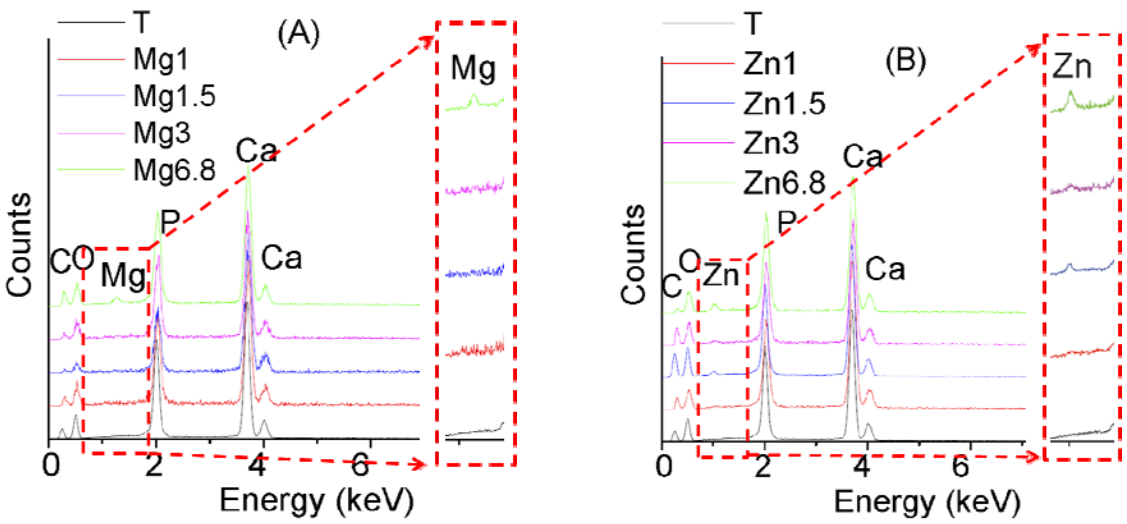

Figure S5. EDX analysis of TCP, Mg-TCP (A) and Zn-TCP (B) powders

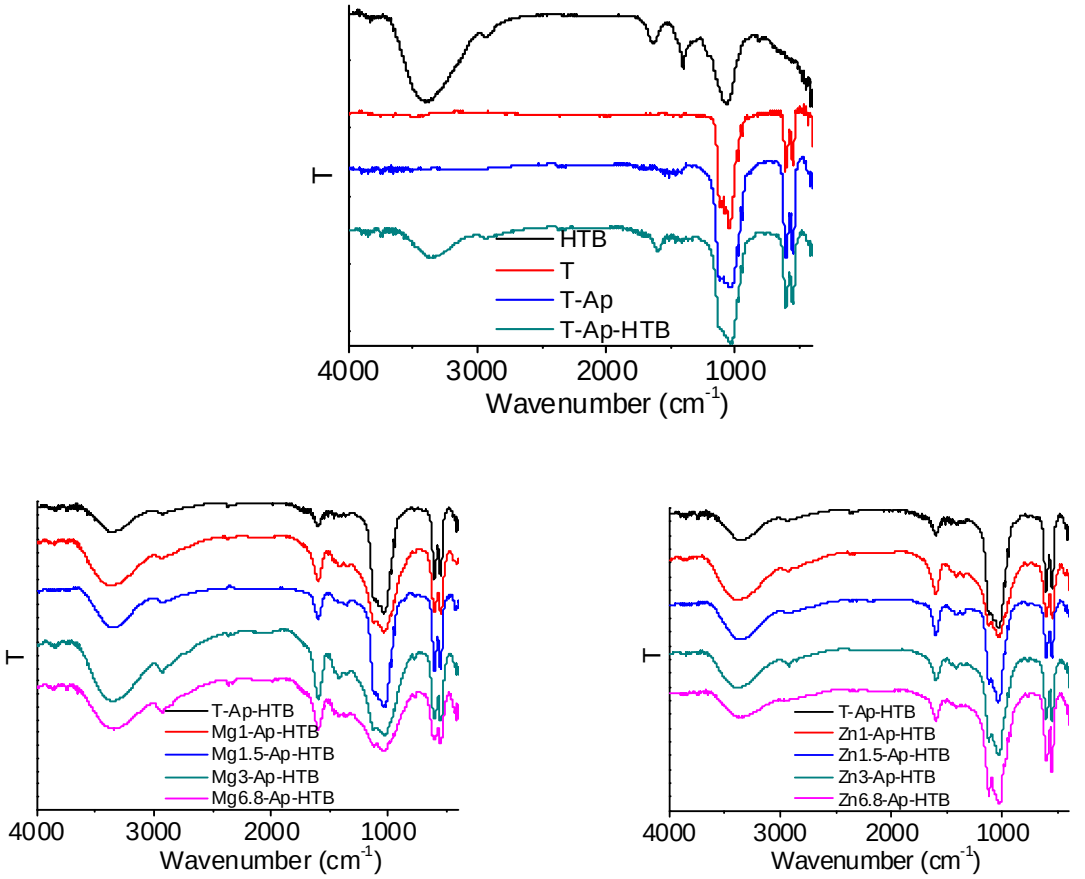

Figure S6. FTIR spectra of HTB, T, T-Ap and T-Ap-HTB and Mg-, Zn-Ap-HTB

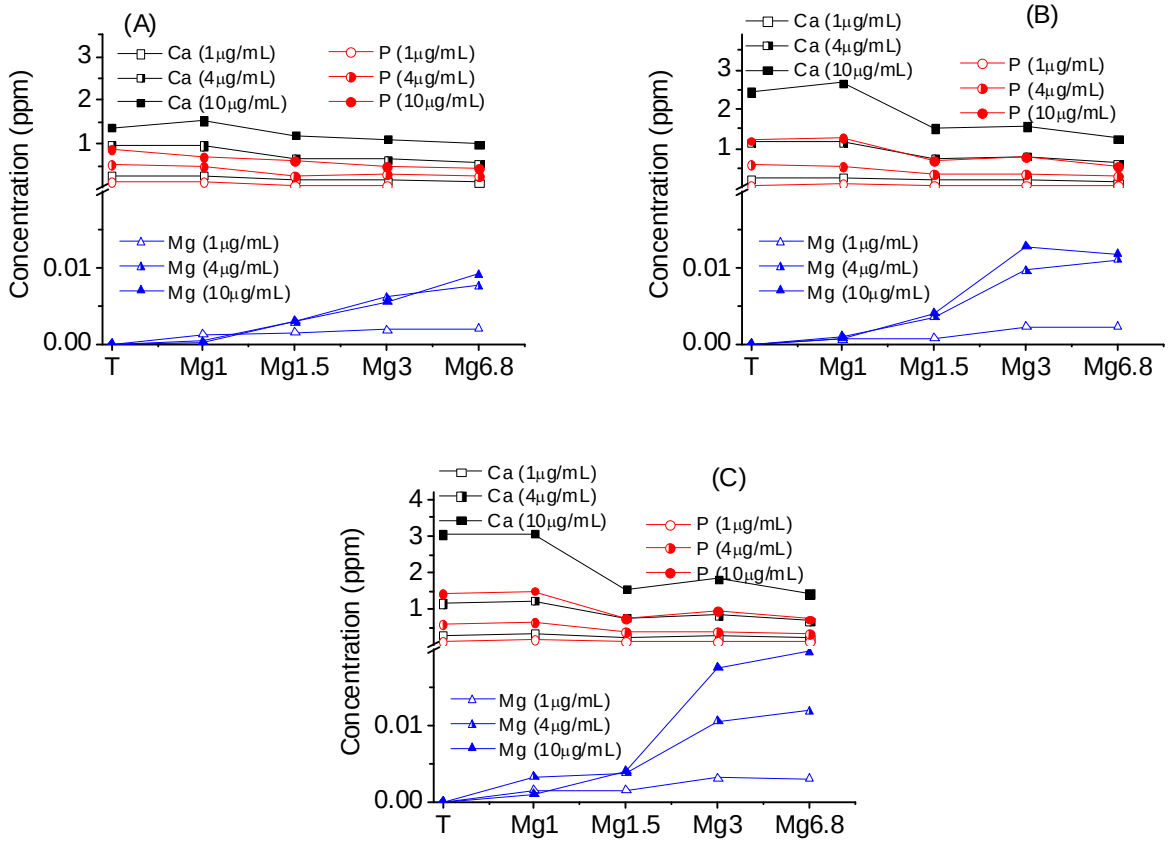

Figure S7. Ca, P and Mg concentrations after immersing 1, 4 and 10 μg/mL of TCP-Ap and MgTCP-Ap in ultrapure water for 5 h (A), 20 h (B) and 42 h (C)

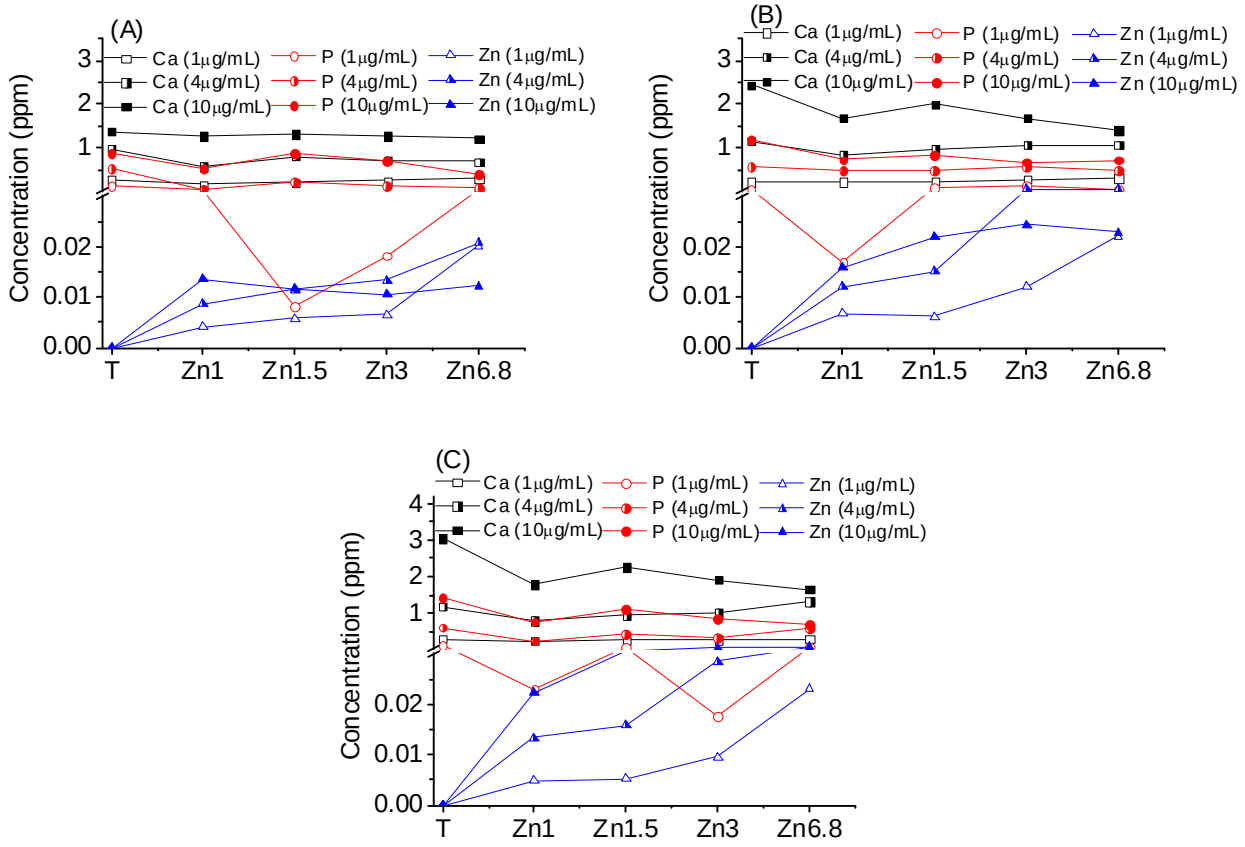

Figure S8. Ca, P and Zn concentrations after immersing 1, 4 and 10 μg/mL of TCP-Ap and ZnTCP-Ap in ultrapure water at 5 h (A), 20 h (B) and 42 h (C)

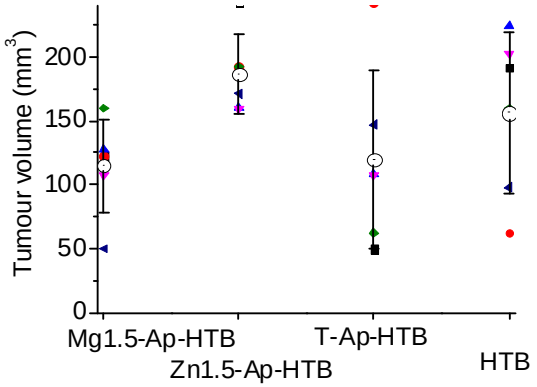

Figure S9. Volume distributions of tumors in each experimental group just before surgical removal from left flanks of mice. Open circles with error bars show mean values and standard deviations of tumor volumes (fist experiment, n=5)

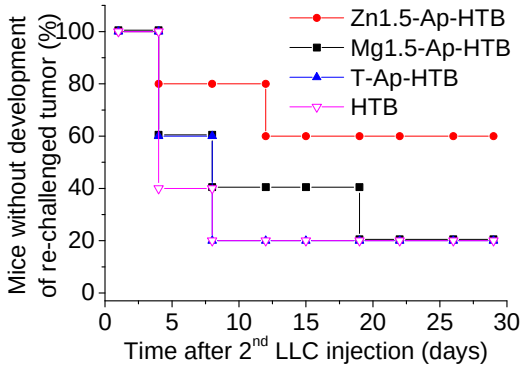

Figure S10. Percent of mice without development of re-challenged tumor on the right flank of the mice over time after re-challenge of LLC cells (fist experiment, n=5)

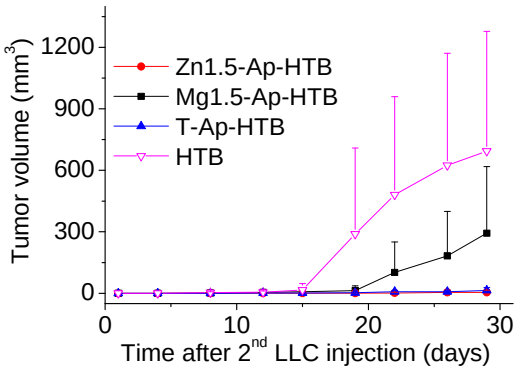

Figure S11. Changes in tumor volume on the right flank of the mice over time after re-challenge of LLC cells (fist experiment, n=5)

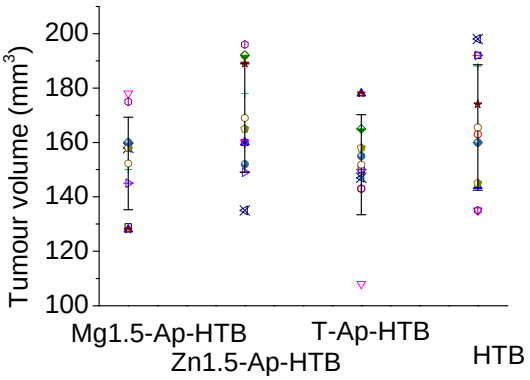

Figure S12. Volume distributions of tumors in each experimental group just before surgical removal from left flanks of mice. Open circles with error bars show mean values and standard deviations of tumor volumes (second experiment, n=12)

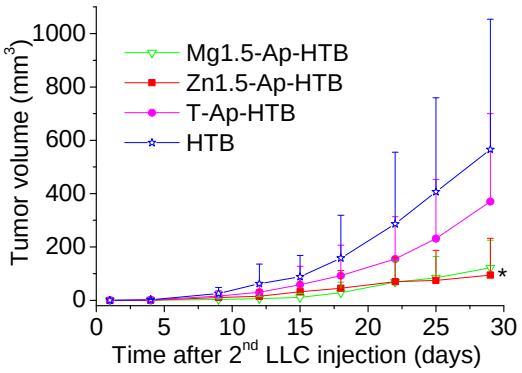

Figure S13. Changes in tumor volume on the right flank of the mice over time after re-challenge of LLC cells (second experiment, n=12)